

Lactide Polymerization with Chiral β -Diketiminato Zinc Complexes

Frédéric Drouin, Paul O. Oguadinma, Todd J. J. Whitehorne, Robert E. Prud'homme, and Frank Schaper*

Département de Chimie, Université de Montréal, 2900 Boulevard E.-Montpetit, Montréal, QC, H3T 1J4, Canada

Received February 25, 2010

N,N'-Di(*S*-phenylethyl)-2-amino-4-iminopent-2-ene, *S,S*-nacnac^{CH(Me)Ph}H, **1a**, and *N,N'*-dibenzyl-2-amino-4-iminopent-2-ene, *nacnac*^{Bn}H, **1b**, react with ZnEt₂ to form the corresponding *nacnac*ZnEt complexes **2a** and **2b**. Neither complex is reactive with 2-propanol or methyl lactate to produce the corresponding alkoxide complexes. In reactions with **2b**, ligand redistribution occurs and *nacnac*^{Bn}Zn was obtained. Reaction of **1a** and **1b** with Zn(N(SiMe₃)₂)₂ yielded *nacnac*ZnN(SiMe₃)₂, **6a** and **6b**. From further reactions with 2-propanol *nacnac*ZnOiPr, **7a** and **7b**, were obtained. Both complexes were catalytically active for polymerization of *rac*-lactide with apparent first-order rate constants of $k_{app} = 0.013\text{--}0.019\text{ min}^{-1}$ and $0.019\text{--}0.038\text{ min}^{-1}$ for **7a** and **7b**, respectively. Obtained polymers were highly heterotactic, with $P_r = 0.84\text{--}0.87$ (**7a**) and $0.65\text{--}0.71$ (**7b**). Analysis of remaining monomer after 75% conversion showed negligible ee and indicates that chiral **7a** does not show enantioselectivity in *rac*-lactide polymerization. Complex **7a**, but not **7b**, catalyzes unselective transesterification of the polymer during and after polymerization. PLA microstructures in polymerizations with **7b** were independent of temperature (23 or 0 °C) or monomer/catalyst ratio (100:1 to 400:1). However, slightly higher P_r values were obtained in the presence of 10–100 equiv of MeCN or pyridine. Complexes *nacnac*^{Bn}Zn, **2b**, **6b**, and **7a** were characterized by an X-ray diffraction study.

Introduction

Polylactide (PLA) finds increasing use as a commodity polymer due to its biodegradability and the possibility of deriving the monomer from renewable resources. Numerous catalyst systems for the polymerization of lactide to PLA have been developed.¹ There is, however, still a remarkable lack of highly active catalyst systems capable of polymerizing *rac*-lactide, the racemic mixture of *R,R*- and *S,S*-lactide, to isotactic PLA, which is the tacticity of highest commercial interest. Typically, Sn-based catalysts display high activities, but no stereoselectivity.² At most, a slight preference for heterotacticity was observed with diketiminato tin complexes.³ Chiral SALEN-based aluminum catalysts give rise to isotactic (or block-isotactic) PLA, but only with low to moderate activity.^{4,5} Mehrkhodavandi and co-workers recently reported a

more active indium system that polymerizes *rac*-lactide with modest isoselectivity ($P_m = 0.53\text{--}0.65$).⁶ Zinc-based catalysts are generally more active than those based on aluminum, but obtaining isotactic enantiopure or stereoblock polymers from *rac*-lactide with these catalysts remains a challenge.

In their seminal work on β -diketiminato zinc complexes, Coates and co-workers obtained highly stereoregular heterotactic PLA⁷ from *rac*-lactide by a chain-end control mechanism, which favors alternating insertion of lactide enantiomers.⁸ In subsequent works, numerous groups varied substitution patterns, denticity, and the metal center (Zn or Mg) of β -diketiminato-based catalysts,^{9–15} but stayed close to the “traditional” framework of a diketiminato ligand with

*Corresponding author. E-mail: Frank.Schaper@umontreal.ca.

(1) Stanford, M. J.; Dove, A. P. *Chem. Soc. Rev.* **2010**, *39*, 486.
Wheaton, C. A.; Hayes, P. G.; Ireland, B. J. *Dalton Trans.* **2009**, 4832.
Chisholm, M. H.; Zhou, Z. J. *Mater. Chem.* **2004**, *14*, 3081.
Dechy-Cabaret, O.; Martin-Vaca, B.; Bourissou, D. *Chem. Rev.* **2004**, *104*, 6147.

(2) Platel, R. H.; Hodgson, L. M.; Williams, C. K. *Polym. Rev. (Philadelphia, PA, U. S.)* **2008**, *48*, 11.

(3) Dove, A. P.; Gibson, V. C.; Marshall, E. L.; White, A. J. P.; Williams, D. J. *Chem. Commun.* **2001**, 283.

(4) Spassky, N.; Wisniewski, M.; Pluta, C.; Le Borgne, A. *Macromol. Chem. Phys.* **1996**, *197*, 2627.
Radano, C. P.; Baker, G. L.; Smith, M. R. *J. Am. Chem. Soc.* **2000**, *122*, 1552.
Ovitt, T. M.; Coates, G. W. *J. Polym. Sci., Part A: Polym. Chem.* **2000**, *38*, 4686.
Ovitt, T. M.; Coates, G. W. *J. Am. Chem. Soc.* **2002**, *124*, 1316.

(5) Isotactic PLA was also obtained in some cases with achiral aluminum catalysts, albeit normally with less stereocontrol. Depending on the ligand, chain-end control for aluminum-based catalysts varies between preferred isotactic and, more rarely, preferred syndiotactic enchainment. Wisniewski, M.; Le Borgne, A.; Spassky, N. *Macromol. Chem. Phys.* **1997**, *198*, 1227.
Nomura, N.; Ishii, R.; Akakura, M.; Aoi, K. *J. Am. Chem. Soc.* **2002**, *124*, 5938.
Hormnirun, P.; Marshall, E. L.; Gibson, V. C.; White, A. J. P.; Williams, D. J. *J. Am. Chem. Soc.* **2004**, *126*, 2688.

(6) Douglas, A. F.; Patrick, B. O.; Mehrkhodavandi, P. *Angew. Chem., Int. Ed.* **2008**, *47*, 2290.

(7) Since the monomer already contains two stereocenters with identical stereochemistry, i.e., an *m*-dyad, it is not possible to obtain syndiotactic PLA from *rac*-lactide. Polymerization with preference for alternating *R,R/S,S* enchainments affords heterotactic PLA with alternating *m*- and *r*-dyads (mr)_n.

(8) Cheng, M.; Attygalle, A. B.; Lobkovsky, E. B.; Coates, G. W. *J. Am. Chem. Soc.* **1999**, *121*, 11583.

(9) Chamberlain, B. M.; Cheng, M.; Moore, D. R.; Ovitt, T. M.; Lobkovsky, E. B.; Coates, G. W. *J. Am. Chem. Soc.* **2001**, *123*, 3229.

(10) Chisholm, M. H.; Huffman, J. C.; Phomphrai, K. *J. Chem. Soc., Dalton Trans.* **2001**, 222.
Chisholm, M. H.; Gallucci, J.; Phomphrai, K. *Inorg. Chem.* **2002**, *41*, 2785.

(11) Chisholm, M. H.; Phomphrai, K. *Inorg. Chim. Acta* **2003**, *350*, 121.

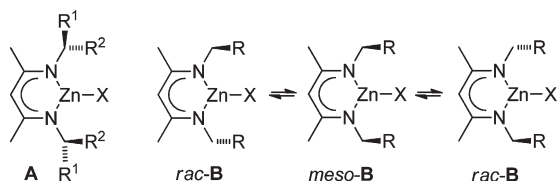
(12) Dove, A. P.; Gibson, V. C.; Marshall, E. L.; White, A. J. P.; Williams, D. J. *Dalton Trans.* **2004**, 570.

(13) Yu, K.; Jones, C. W. *J. Catal.* **2004**, *222*, 558.
Sanchez-Barba, L. F.; Hughes, D. L.; Humphrey, S. M.; Bochmann, M. *Organometallics* **2006**, *25*, 1012.
Ayala, C. N.; Chisholm, M. H.; Gallucci, J. C.; Krempner, C. *Dalton Trans.* **2009**, 9237.

(14) Chen, H.-Y.; Huang, B.-H.; Lin, C.-C. *Macromolecules* **2005**, *38*, 5400.

(15) Chisholm, M. H.; Gallucci, J. C.; Phomphrai, K. *Inorg. Chem.* **2005**, *44*, 8004.

Scheme 1



aromatic N-substituents. In general, heterotactic PLAs with different degrees of stereocontrol were obtained. In an attempt to gain access to C_1 - or C_2 -symmetric catalysts and to overcome chain-end-controlled monomer enchainment with a catalytic-site control mechanism, Chisholm et al. investigated diketiminato zinc and magnesium complexes with monosubstituted aryl N-substituents.^{11,15} While isomerization around the N-aryl bond was slow compared to polymerization, the C_2 -symmetric *meso* rotamer proved to be the most active and led to heterotactic PLA. Similar studies of Dove et al. using a C_1 -symmetric ligand yielded nearly atactic PLA.¹² Mehrkhodavandi and co-workers incorporated the chiral cyclohexylenediamine framework, used successfully on indium as the central metal, in tetrahedral zinc complexes, but obtained only low activities and isotacticities.¹⁶

We recently became interested in derivatives of diketiminato ligands with aliphatic N-substituents. In contrast to N-aryl diketiminates, these ligands lend themselves more easily to generate a C_2 -symmetric environment, and we were able to prepare a chiral derivative from chiral amines and the respective copper and zirconium complexes.^{17–19} Use of diketiminato ligands with aliphatic substituents on nitrogen offers access to complexes that either are inherently chiral (Scheme 1, A) or form chiral rotamers (Scheme 1, B). We will present here the synthesis of two examples for A and B and their performance in the polymerization of *rac*-lactide.

Results and Discussion

***nacnac*ZnEt Complexes.**²⁰ Following a protocol reported for *nacnac*^{Ar}ZnEt,²¹ reaction of diketimines *S,S*-*nacnac*^{CH(Me)Ph}H, **1a**, and *nacnac*^{Bn}H, **1b**, with ZnEt₂ yielded the corresponding zinc ethyl complexes **2a** and **2b** in 86% and 95% yield, respectively (Scheme 2). Both complexes display similar NMR spectra: a C_2/C_2v -symmetric set of resonances for the diketiminato ligand, a triplet at 1.1–1.3 ppm for ZnCH₂Me, and a quartet at 0.3–0.4 ppm for ZnCH₂Me. As in most asymmetric zinc ethyl complexes, the two diastereotopic ZnCH₂ hydrogen atoms in **2a** are not differentiated and appear as a single quartet. In contrast to other diketimine zinc alkyl complexes, **2b** forms a dimer in the solid state (Figure 1, only one of two independent molecules is shown). The compound is present as its *meso* rotamer, with the N-benzyl substituents in a *syn* orientation on the same side of the ligand mean plane. This allows the approach of a second molecule of *meso*-**2b**, which is related to

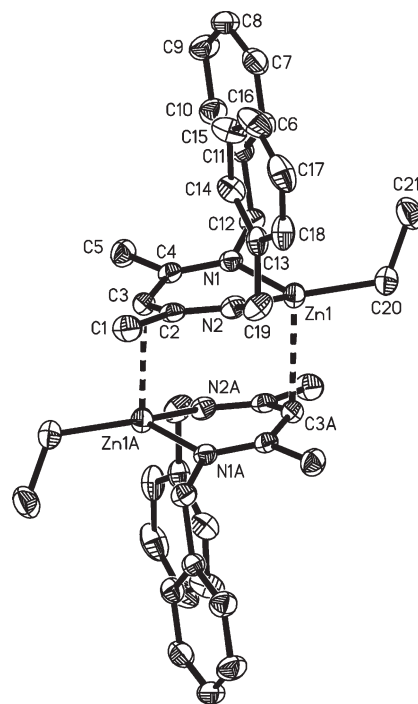
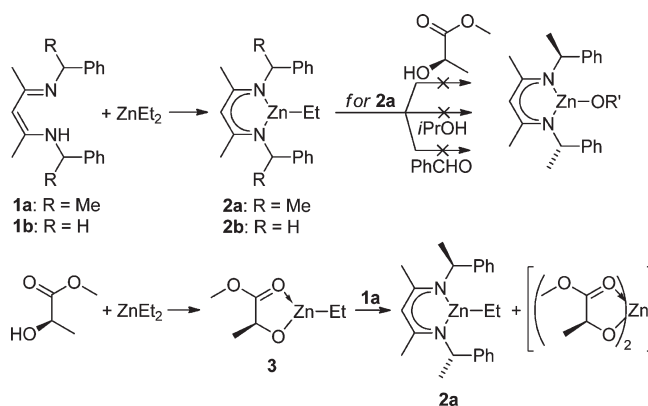


Figure 1. X-ray crystal structure of **2b**. Hydrogen atoms have been omitted for clarity. The second independent molecule in the unit cell (Zn2, N3, N4, C31–C51) of essentially identical geometry is not shown. Thermal ellipsoids are drawn at the 50% probability level.

Scheme 2



the first by a crystallographic inversion center and coordinates with the central carbon atom in the ligand backbone (C3 or C33) to Zn. Such a close approach of the two ligand mean planes (3.1 Å) is not possible with *N*-aryl substituents for steric reasons. Consequently, *nacnac*^{Ar}ZnR complexes display either three-coordinated Zn centers^{12,22–24} or coordination of an additional donor ligand (RCN, Py) to Zn.²⁵ Zn–C distances (Table 1) are at the higher end of the range observed for *nacnac*^{Ar}ZnEt complexes (1.95–1.99 Å).^{12,22,24,25} While

(16) Labourdette, G.; Lee, D. J.; Patrick, B. O.; Ezhova, M. B.; Mehrkhodavandi, P. *Organometallics* **2009**, *28*, 1309.

(17) Buch, F.; Harder, S. Z. *Naturforsch., B: Chem. Sci.* **2008**, *63*, 169.

(18) Oguadinma, P. O.; Schaper, F. *Organometallics* **2009**, *28*, 4089.

(19) El-Zoghbi, I.; Latreche, S.; Schaper, F. *Organometallics* **2010**, *29*, 1551.

(20) Diketiminato zinc complexes might exist as monomers or dimers in the solid state or in solution. For the sake of simplicity, all complexes are described in monomeric form.

(21) Cheng, M.; Lobkovsky, E. B.; Coates, G. W. *J. Am. Chem. Soc.* **1998**, *120*, 11018.

(22) Cheng, M.; Moore, D. R.; Reczek, J. J.; Chamberlain, B. M.; Lobkovsky, E. B.; Coates, G. W. *J. Am. Chem. Soc.* **2001**, *123*, 8738.

(23) Prust, J.; Stasch, A.; Zheng, W.; Roesky, H. W.; Alexopoulos, E.; Uson, I.; Bohler, D.; Schuchardt, T. *Organometallics* **2001**, *20*, 3825.

(24) Cole, S. C.; Coles, M. P.; Hitchcock, P. B. *Organometallics* **2004**, *23*, 5159. Piesik, D. F. J.; Range, S.; Harder, S. *Organometallics* **2008**, *27*, 6178.

(25) Allen, S. D.; Moore, D. R.; Lobkovsky, E. B.; Coates, G. W. *J. Organomet. Chem.* **2003**, *683*, 137. Lee, S. Y.; Na, S. J.; Kwon, H. Y.; Lee, B. Y.; Kang, S. O. *Organometallics* **2004**, *23*, 5382.

Table 1. Selected Bond Distances [Å] and Bond Angles [deg] for Crystal Structures of **4**, **6b**, and **7a**

	2b	4	6b	7a
Zn1–N1/Zn2–N3	1.990(1)/2.005(1)	1.983(1)	1.942(2)	1.984(2)/1.988(2)
Zn1–N2/Zn2–N4	1.988(1)/1.996(1)	1.989(1)	1.940(2)	2.007(2)/1.993(2)
Zn–X ^a	1.984(2)/1.982(3)		1.890(2)	1.971(2)–2.023(2)
N–Zn–N ^b	95.06(6), 95.28(6)	97.93(7), 98.27(7)	99.61(7)	99.21(8), 99.68(8)
N–Zn–X ^c	119.8(1)–132.8(1)	114.80(5), 116.08(5)	129.99(7), 130.39(7)	108.91(8)–130.32(8)
O1–Zn–O2				82.52(6), 82.43(6)

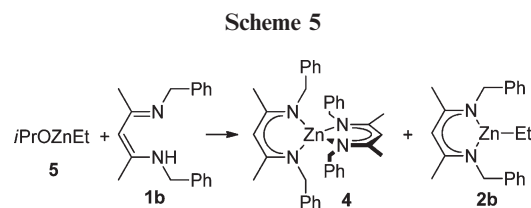
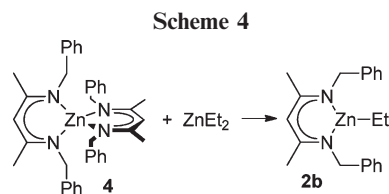
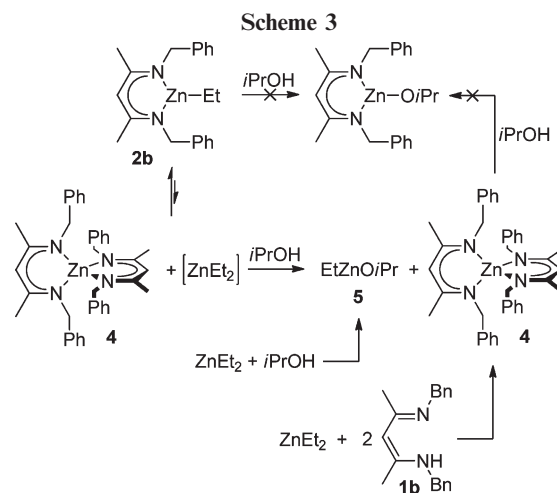
^a **2b**: Zn1–C20, Zn2–C50a. **6b**: Zn1–N3. **7a**: Zn1/2–O1/2. ^b Diketiminato bite angle, **2b**: N1–Zn1–N2, N3–Zn2–N4; **4**: N1–Zn1–N1A, N2–Zn1–N2A; **6b**: N1–Zn1–N2; **7a**: N1–Zn1–N2, N3–Zn2–N4. ^c **2b**: X = C20, C50a. **4**: N1–Zn1–N2. **6b**: N1–Zn1–N3, N2–Zn1–N3. **7a**: X = O1, O2.

clearly present, coordination of the backbone carbon atom C3/C33 to Zn is weak (Zn–C: 2.582(2) and 2.539(2) Å) and the Zn atom is only slightly distorted from its trigonal-planar coordination with C3/C33–Zn–C_{Et}/N angles of 96–106°, the sum of the N–Zn–N/C_{Et} close to 360° (349° and 353°), and displacements of Zn out of the N/N/C_{Et} plane of less than 0.4 Å.

Since *nacnac*ZnEt complexes have been shown to be slow initiators of lactide polymerization,⁹ we attempted to replace the ethyl group by alkoxide. Reaction of **2a** or **2b** with either 2-propanol, methanol, or *S*-methyl lactate did not yield the respective *nacnac*ZnOR complexes in a variety of solvents (toluene, C₆D₆, hexane, THF), at –80 °C or room temperature, or with varying order of reagent addition. For **2a**, heating or prolonged reaction times yielded the free ligand **1a** as the only diketimine-containing species next to unreacted starting material. Complex **2a** proved also to be unreactive toward insertion of benzaldehyde (60 °C, 2 h, C₆D₆). In an attempt to reverse the order of ligand coordination, we reacted **3**, prepared from *S*-methyl lactate and ZnEt₂, with **1a** (Scheme 2). Only starting material was observed after 24 h of reaction in toluene at room temperature, accompanied by small amounts (5%) of **2a**. Following the reaction at 65 °C for 24 h by NMR spectroscopy showed slowly increasing amounts of **2a** together with some insoluble precipitate, but no indication for the formation of the desired diketiminato zinc lactate complex. Complex **2a** is most likely formed by a ligand redistribution of **3** to give the, probably insoluble, zinc bislactate and ZnEt₂, which in turn reacts with diketimine **1a**.

¹H NMR spectra of the reaction of **2b** with 2-propanol displayed several new signals, which could by independent synthesis be assigned to the bis(*nacnac*) zinc complex **4** and to ethyl zinc isopropanolate, **5**²⁶ (Scheme 3). Again, no formation of *nacnac*^{Bn}ZnOiPr was observed under a variety of reaction conditions. Formation of a homoleptic bis(*nacnac*) complex was observed only with *nacnac*^{Bn}, but not in reactions with *nacnac*^{CH(Me)Ph}, which can be attributed to the sterically more demanding nature of the latter ligand. Indeed, attempts to prepare (*nacnac*^{CH(Me)Ph})₂Zn analogous to **4** from ZnEt₂ and excess **1a** yielded only the heteroleptic complex **2a**, next to unreacted diketimine.

Formation of homoleptic L₂Zn complexes upon reaction of LZnEt with alcohol has been reported previously for sterically undemanding *nacnac*^{Ar} and tris(pyrazolyl)borate ligands.^{14,22,27} A possible mechanism is protonation of the diketiminato ligand by 2-propanol to form **5** and trapping of *nacnac*^{Bn}H by **2b** to yield **4**. Alternatively, **2b** might undergo reversible ligand redistribution to **4** and ZnEt₂, the latter irreversibly reacting with 2-propanol to form **5**. Since a solution of ZnEt₂ in C₆D₆ reacted



completely with **4** in less than 30 min to the heteroleptic complex **2b** (Scheme 4), the inverse reaction, i.e., the ligand redistribution of **2b**, seems feasible. Given the fact that protonation of the diketiminato ligand in **2a** by 2-propanol occurred only partially and upon heating, we believe the latter mechanism to be responsible for the observed reaction products (Scheme 3).²⁸

¹H NMR spectra of reactions of **1b** with *i*PrOZnEt showed mixtures indicative of ligand exchange reactions, which contained **1b**, **2b**, **4**, and an insoluble product, most likely Zn(OiPr)₂, in varying amounts, but no evidence for *nacnac*^{Bn}ZnOiPr (Scheme 5). Attempted protonation of **4** with *i*PrOH yielded only mixtures of **4** and small amounts of the protonated ligand **1b**.

(26) Herolds, R. J.; Aggarwal, L.; Neff, V. *Can. J. Chem.* **1963**, *41*, 1368.

(27) Looney, A.; Han, R.; Gorrell, I. B.; Cornebise, M.; Yoon, K.; Parkin, G.; Rheingold, A. L. *Organometallics* **2002**, *14*, 274.

(28) Formation of **4** was observed in some cases when solutions of **2b** are kept for extended periods of time. Varying amounts of **4** indicate that **2b** is not inherently prone to disproportionation and that in the absence of alcohol protic impurities might be required to remove ZnEt₂ from the equilibrium.

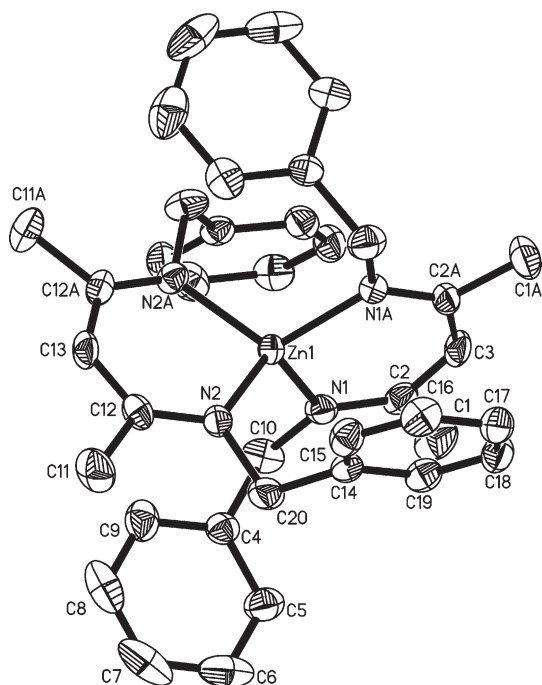


Figure 2. X-ray crystal structure of **4**. Hydrogen atoms have been omitted for clarity. Thermal ellipsoids are drawn at the 50% probability level.

Crystals suitable for an X-ray diffraction study were obtained for **4** (Figure 2, Table 1). The structure of **4**, which crystallizes on a crystallographic C_2 -axis, is close to S_4 symmetry with the benzyl substituents oriented in a *rac* conformation on opposing sides of the ligand mean plane (cf. the *meso* conformation observed in **2a**, Figure 1). The phenyl rings are positioned above the benzylic CH_2 group of the opposite ligand in a close $CH-\pi$ interaction (2.8 Å). Short intermolecular $\pi-\pi$ interactions (3.6 Å) are observed between the C14–C19 rings of adjacent molecules. In contrast to *nacnac*^{Ar}₂Zn complexes,^{22,29} which show the typical boat-like distortion of diketimate metal complexes as a consequence of steric congestion, the Zn atom in **4** is located in the mean plane of the diketimate ligands. This is in line with observations for *nacnac*^{Bn}Cu complexes: diketimate ligands with primary alkyl substituents on nitrogen are sterically less demanding than their counterparts with *N*-aryl substituents.³⁰ In agreement with this, Zn–N distances (1.983(1) and 1.989(1) Å) are shorter and the coordination geometry around nitrogen is more symmetric (differences in N–Zn–N angles, where N_A and N_B are of a different diketimate ligands: $\Delta(N_A-Zn-N_B) < 2^\circ$) than in *nacnac*^{Ar}₂Zn complexes (Zn–N: 1.99–2.04 Å, $\Delta(N_A-Zn-N_B) = 12-26^\circ$).^{22,29}

2-Propanol has been reported not to react (or to react only to a minor extent) with the Zn–Et group in *nacnac*^{dipp}ZnEt (dipp = 2,6-diisopropylphenyl),²² (NNO)ZnEt (NNO = diaminophenol)¹⁶ or even in *i*PrOZnEt.²⁶ Labourdette et al. reported that protonation of (NNO)ZnEt was possible with phenols,¹⁶ but given the slow initiation of lactide polymerization by [Zn]OAr, we did not pursue this pathway further.

***nacnac*Zn(amide) and *nacnac*ZnOiPr Complexes.** Following the protocol established by Coates and co-workers,⁸ we attempted the synthesis of the targeted complexes by

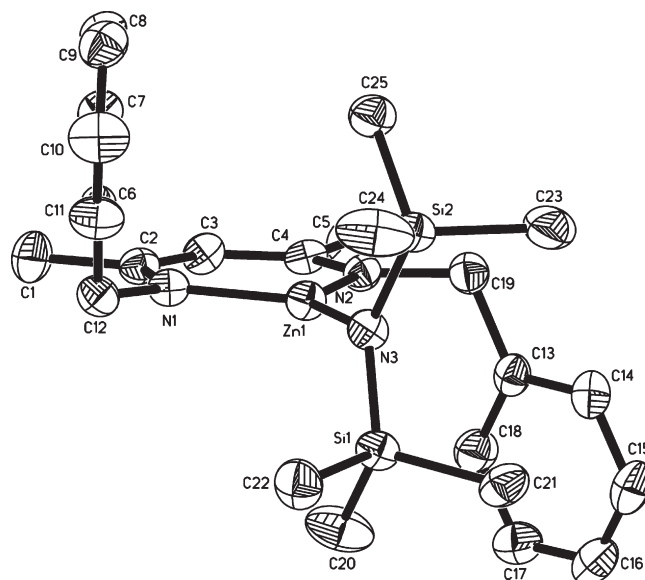
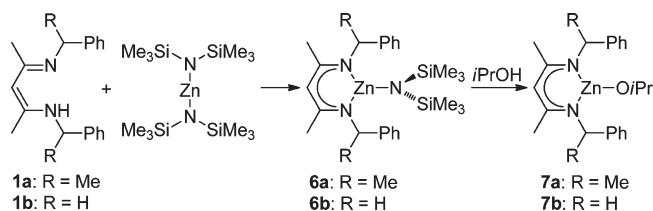


Figure 3. X-ray crystal structure of **6b**. Hydrogen atoms are omitted for clarity. Thermal ellipsoids are drawn at the 50% probability level.

Scheme 6



protonation of the respective zinc amides. Reaction of Zn–{N(SiMe₃)₂}₂ with ligands **1a** and **1b** afforded the amide complexes **6a** and **6b** in good yields (Scheme 6). Complex **6a** was obtained as a highly viscous oil and could not be purified. The impurities, mainly HN(SiMe₃)₂ and unreacted **1a**, did not interfere in the subsequent reaction with 2-propanol. The crystal structure of **6b** (Figure 3, Table 1) shows again a more symmetric complex, when compared to its *nacnac*^{Ar}ZnN(SiMe₃)₂ analogues ($\Delta(Zn-N1/2)$: **6b**, < 0.01 Å; *nacnac*^{Ar}, 0.02–0.04 Å; $\Delta(N-Zn-N3)$: **6b**, < 0.5°; *nacnac*^{Ar}, 2–8°).^{12,15,22} The Zn–N3 bond is found in the mean plane of the diketimate ligand, without the boat-like distortion observed in *nacnac*^{Ar}ZnN(SiMe₃)₂.^{12,15,22} The N(SiMe₃)₂ fragment is nearly perpendicular (82°) to the mean ligand plane, indicating only small interactions between the *anti*-orientated benzyl ligands and the trimethylsilyl substituents.

Reaction of **6a** or **6b** with 2-propanol cleanly generated the corresponding alkoxide complexes **7a** and **7b**, respectively (Scheme 6). The presence of the chiral ligand in **7a** is now visible in the slight splitting of the isopropyl methyl groups into two signals in the ¹H and ¹³C NMR spectra. Complex **7b**, on the other hand, showed NMR spectra of apparent C_{2v} symmetry: one singlet is observed for the NCH₂Ph hydrogen atoms in the ¹H NMR and the methyl groups of the OiPr ligand appear as one doublet in the ¹H and one resonance in the ¹³C NMR spectra. Rotation around the N–Bn bond is thus fast on the NMR time scale for **7b**. Barriers of rotation around the N–C bond seem to be strongly dependent on the steric demand of the substituent. A mixture of *rac* and *meso* rotamers has been observed in NMR spectra of *nacnac*^{Ar}ZnX complexes with

(29) Peng, Y.-L.; Hsueh, M.-L.; Lin, C.-C. *Acta Crystallogr., Sect. E* **2007**, *63*, m2388.

(30) Oguadinma, P. O.; Schaper, F. *Organometallics* **2009**, *28*, 6721.

mono-*t*Bu-substituted aryl substituents,¹¹ while fast rotation was observed for their monomethoxy-substituted analogues.¹⁵ Despite the tendency of **2b** to form the homoleptic complex **4** in the presence of alcohol, solutions of **7b** in C₆D₆ showed no evidence of ligand redistribution over a period of 7 days at room temperature.

The crystal structure of **7a** displays a dimeric zinc complex with bridging isopropanolate ligands (Figure 4). Formation of a dimeric complex introduces significant steric strain, and the secondary alkyl substituent seems to be too bulky to accommodate the formation of the dimer in its lowest energy conformation, i.e., with the phenyl groups in an *anti* conformation and the CH(Me)Ph hydrogen atoms oriented toward the ligand backbone. Instead, rotations around the N2–C20 and the N4–C41 bonds orient the CH(Me)Ph hydrogen atoms toward each other and lead to a *syn* conformation of the phenyl groups on the same side of the ligand mean plane. Accordingly, the dimer distorts to accommodate the CH(Me)Ph groups in their normal conformation with a N1–N3 distance of 6.0 Å, while the rotated CH(Me)Ph groups allow a closer approach of the two ligands with $d(\text{N2–N4}) = 5.1$ Å. Zn–N and Zn–O bond lengths are comparable to those observed in analogous complexes with *nacnac*^{Ar} ligands, while N–Zn–N angles are slightly larger (Table 1, *nacnac*^{Ar}: Zn–N: 2.00–2.07 Å, Zn–O: 1.95–2.02 Å, N–Zn–N: 94.8–96.0°).^{8,9,31} As a consequence of its distorted structure, **7a** displays a high variation in Zn–O bond lengths ($\Delta(\text{Zn–O}) = 0.05$ Å, *nacnac*^{Ar}: $\Delta(\text{Zn–O}) = 0–0.06$ Å). While there was no evidence for the rotation of a secondary alkyl substituent around the N–C bond in planar *nacnac*^RCuL (R = *i*Pr, CH(Me)Ph)^{18,32} or *nacnac*^{iPr}PdX (X = *nacnac*^{iPr}, allyl)³³ complexes, it was previously observed in octahedral *nacnac*^RZrCl₂ (R = Cy, CH(Me)Ph)¹⁹ and square-pyramidal *nacnac*^{iPr}TiX₃ complexes.³⁴

Lactide Polymerization. Both complexes **7a** and **7b** were active for the polymerization of *rac*-lactide in CH₂Cl₂.³⁵ Complete conversion was achieved after 3 and 1.5 h, respectively (>95%, 7/lactide = 1:300, [7] = 1.5–2.0 mM, 23 °C). Analyses of the polymer microstructure revealed that both complexes exhibit a strong preference for alternating insertion of *RR*- and *SS*-enantiomers, leading to predominantly heterotactic PLA ($P_r = 0.84–0.87$ and $0.65–0.71$ for **7a** and **7b**, respectively, where P_r is the probability of forming an *r*-dyad by insertion).⁷ Similar preferences with *C_s*-symmetric diketiminate zinc complexes have been attributed to chain-end control.⁸ Narrow polydispersities of $M_w/M_n = 1.1$ for selected samples are consistent with a living polymerization mechanism, as expected for this catalyst system. Polymer molecular weights are slightly higher than expected (5–25%), probably due to catalyst decomposition. Determination of reaction kinetics with **7a** and **7b** showed the expected first-order dependence on monomer concentration. Pseudo-first-order rate constants of $k_{\text{app}} = 0.019–0.038$ min^{−1} were found for **7b**, which are comparable to $k_{\text{app}} = 0.054$ min^{−1} observed for *nacnac*^{dipp}ZnOiPr under comparable conditions ([Zn]/lactide = 1:490, [Zn] = 2.1 mM).⁹

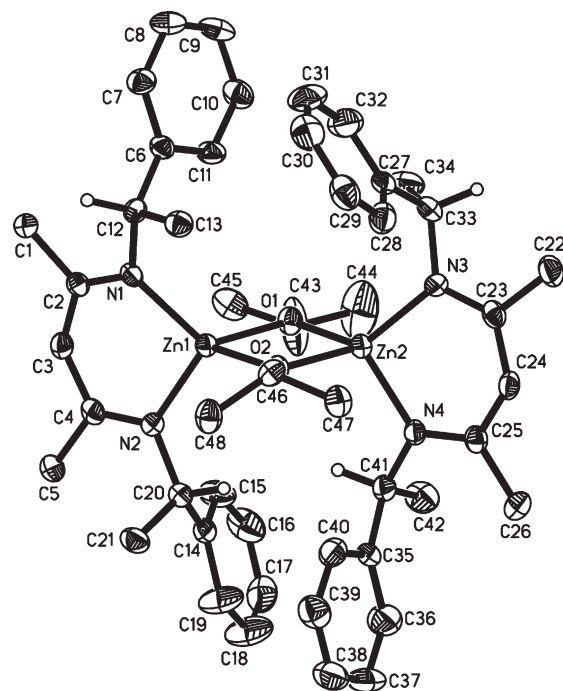


Figure 4. X-ray crystal structure of **7a**. Most hydrogen atoms are omitted for clarity. Thermal ellipsoids are drawn at the 50% probability level.

Table 2. *rac*-Lactide Polymerizations (CH₂Cl₂, 23 °C) with **7a**

	[Zn] (mM)	[Zn]/[lactide]	<i>T</i> (°C)	k_{app} (min ^{−1})	P_r^a
#1	1.8	1:300	23	0.019(2)	0.85
#2	1.8	1:300	23	0.015(1)	0.85 ^b
#3	1.9	1:300	23	0.016(1)	0.87 ^c
#4	1.7	1:300	23	0.016(1)	0.85 ^d
#5	1.7	1:200	23		0.84
#6	1.7	1:200	23	0.019(2)	0.88 ^d
#7	1.7	1:100	23	0.013(1)	0.86 ^d

^a Determined after complete conversion of monomer from decoupled ¹H NMR by $P_r = 2I_1/(I_1 + I_2)$, with $I_1 = 5.20–5.25$ ppm (*rmr*, *mnr*/*rrm*), $I_2 = 5.13–5.20$ ppm (*mnr*/*rrm*, *mmm*, *mrm*). ^b $M_n = 53\,000$, $M_w/M_n = 1.1$. ^c $M_n = 58\,200$, $M_w/M_n = 1.1$. ^d After 75–85% conversion.

The sterically more congested **7a** displays a reduced polymerization rate constant of $k_{\text{app}} = 0.013–0.019$ min^{−1} (Table 2) and possesses a short induction period of ca. 10 min (Figure 5).

Samples were taken in regular intervals from polymerizations with **7a**, and the microstructure of the polymer was analyzed. As expected, the obtained polymer microstructure is independent of the **7a**/lactide ratio (Table 2, **7a**/lactide = 1:100 to 1:300). The value of P_r , determined from decoupled ¹H NMR spectra (Table 2), decreased from around $P_r \approx 0.90$ at 10% conversion to $P_r = 0.84–0.86$ at 95% conversion (Figure 5). Partial kinetic resolution by enantioselective polymerization cannot explain the gradual decrease of P_r during polymerization. Nevertheless, we analyzed the remaining *rac*-lactide monomer after 75–77% conversion (**7a**/lactide = 1:300) by polarimetry and found negligible enantiomeric excesses of less than 1%. There is thus no preferential insertion of one enantiomer and the chiral N-substituent in **7a** does not impart any enantioselectivity in the polymerization of *rac*-lactide.

If a second batch of 200 equiv of monomer is added to polymerizations of lactide with **7a** (CDCl₃, **7a**/lactide = 1:200) after either 2 or 4 h, the monomer is consumed with essentially

(31) Marsh, R. E.; Clemente, D. A. *Inorg. Chim. Acta* **2007**, *360*, 4017.

(32) Oguadinma, P. O.; Schaper, F. *Can. J. Chem.* **2009**, accepted.

(33) Tian, X.; Goddard, R.; Pörschke, K. R. *Organometallics* **2006**, *25*, 5854.

(34) Nikiforov, G. B.; Roesky, H. W.; Magull, J.; Labahn, T.; Vidovic, D.; Noltemeyer, M.; Schmidt, H.-G.; Hosmane, N. S. *Polyhedron* **2003**, *22*, 2669.

(35) Only complexes **7a** and **7b** were investigated in detail. Amide complex **6b** polymerized *rac*-lactide with lower activity (k_{app} smaller by a factor of 6) but identical stereoselectivity compared to **7b**. Since **6a** was not obtained in pure form, it was not tested for polymerization.

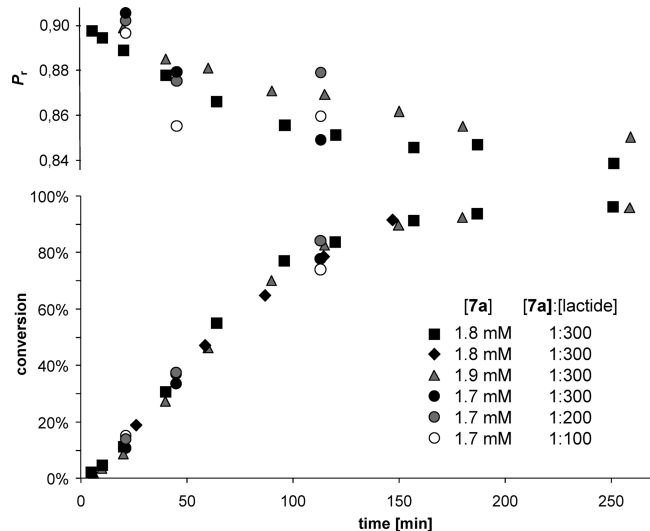


Figure 5. Dependence of conversion and probability of alternating *R,R/S,S*-enchainment (P_r) on polymerization time.

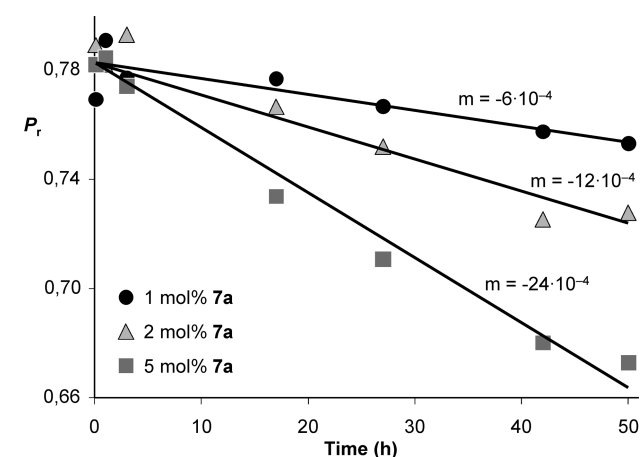


Figure 6. Apparent decrease of P_r in PLA treated with **7a**, determined from decoupled ^1H NMR by $P_r = 2(I_{\text{rmm}} + I_{\text{mmr/rmm}})/I_{\text{total}}$, presuming the absence of *rr*-triads.

identical activity k_{app} and stereoselectivity P_r (see Supporting Information). Decomposition of **7a** during polymerization to an active, but unselective species can thus also be excluded as a reason for the apparent decrease of P_r .

An apparent decrease in P_r was also observed when samples of precipitated and washed PLA were combined with 1, 2, or 5 mol % **7a** (relative to mol monomer in PLA) and followed for several days by NMR (CDCl_3 , room temperature). The change in P_r correlated reasonably with the amount of **7a** added (Figure 6). Analyses of the carbonyl and methine regions in the ^{13}C NMR spectra showed a decrease in *mrm*- and *rmm*-tetrads and an increase in *mmm*-tetrads (Table 3). At the same time, resonances associated with *rrr*- and *rrm/mrr*-tetrads were observed, which cannot be obtained from polymerizations of *rac*-lactide (Figure 7, Table 3). The observed apparent decrease in P_r during polymerizations with **7a** can thus be attributed to an unselective transesterification of PLA, catalyzed by **7a**. The appearance of *rr*-triads, which overlap in the decoupled ^1H NMR spectra, employed for the determination of P_r , with the *mmm* and *mrm* resonances, is responsible for the apparent increase in isotacticity.

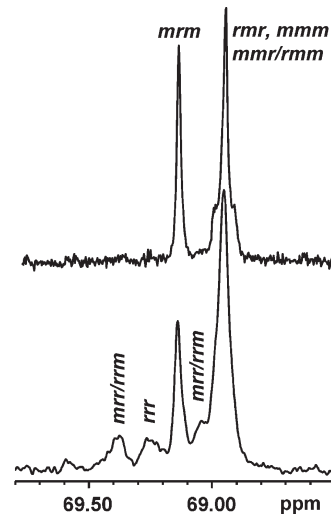


Figure 7. Methine region of PLA $^{13}\text{C}\{^1\text{H}\}$ NMR spectra before (top) and after (bottom) treatment with 5% **7a** for 4 days.

Table 3. Changes in Tetrad Distribution of PLA after Exposure to **7a** for 4 days (determined from ^{13}C NMR spectra)

	PLA	1 mol % 7a	5 mol % 7a
P_r^a	0.78	0.72	0.55
% <i>mmm</i>	13	16	25
% <i>mrm</i> + <i>rmm</i> ^b	17	18	17
% <i>mrm</i>	39	32	20
% <i>rmm</i>	30	29	13
% <i>mrr</i> + <i>rrm</i> ^b	0	3	17
% <i>rrr</i>	0	2	8
% <i>m</i>	61	60	59

^a P_r calculated from decoupled ^1H spectra, presuming the absence of *rr*-triads. ^b Both tetrads were assumed to have equal intensity.

Table 4. *rac*-Lactide Polymerizations (CH_2Cl_2) with **7b**

	[Zn] (mM)	[Zn]/[lactide]	T ($^\circ\text{C}$)	k_{app} (min^{-1})	P_r^a
#1	1.9	1:100	23	0.025(1)	0.65–0.68 ^b
#2	1.7	1:200	23	0.038(1)	0.66
#3	1.9	1:200	23	0.024(5)	0.67–0.68 ^{b,c}
#4	2.0	1:300	23	0.035(3)	0.68 ^d
#5	1.9	1:400	23	0.019(5)	0.68–0.71 ^b
#6	1.7	1:300	0		0.68

^a Determined from decoupled ^1H NMR by $P_r = 2I_1/(I_1 + I_2)$, with $I_1 = 5.20\text{--}5.25$ ppm (*rmm*, *mmr/rmm*), $I_2 = 5.13\text{--}5.20$ ppm (*mmr/rmm*, *mmm*, *mrm*). ^b Polymer samples precipitated after 12, 30, and 65 min. ^c $M_n = 35\,900$, $M_w/M_n = 1.1$. ^d $M_n = 45\,500$, $M_w/M_n = 1.1$.

Polymerizations with **7b** did not show the time-dependent change in P_r observed for **7a**, but displayed in general lower P_r values (Table 4). The reduced stereocontrol with **7b** might be due to an increased tendency to stereoerrors with a less bulky ligand, due to a preference for isotactic monomer enchainment by the chiral rotamers of **7b** or due to the formation of $\text{Zn}(\text{O}i\text{Pr})_2$ by ligand redistribution of **7b** into **4** and $\text{Zn}(\text{O}i\text{Pr})_2$ (cf. Scheme 3). Zinc diisopropanolate is an active, but unselective catalyst for the polymerization of *rac*-lactide ($P_r = 0.5$).³⁶ Since mixtures of **7b** and 50 equiv of *rac*-lactide in CD_2Cl_2 , followed by ^1H NMR spectroscopy, showed only traces of **4** appearing several hours after polymerization was completed, we doubt that ligand redistribution to **4** and $\text{Zn}(\text{O}i\text{Pr})_2$ occurs to any significant extent during polymerizations with **7b**.

(36) Claverie, J. *Personal communication*, Université de Québec et Montréal, Canada, 2009.

Table 5. Influence of the Presence of Additional Lewis Base in Lactide Polymerizations with **7b (CDCl₃, [**7b**] = 1.9 mM, **7b**/lactide = 1:300, ambient temperature)**

L	L/Zn	k_{app}^a (min ⁻¹)	P_r^b
THF	0	0.03	0.63
	10	0.03	0.63
	100	0.03	0.64
	1000	0.02	0.70
MeCN	0	0.03	0.63–0.64
	1	0.03	0.63
	10	0.02	0.63–0.64
	100	0.01	0.65–0.67
pyridine	0	0.03	0.63–0.64
	1	0.03	0.64–0.65
	10	0.03	0.70–0.71
	100	no reaction	

^a k_{app} was estimated from conversions after 5–10, 60–90, and 120–140 min. ^bDetermined after 5–10, 60–90, and 120–140 min from decoupled ¹H NMR by $P_r = 2I(rmr + mnr/rmm)/I(\text{total})$.

Polymerization at 0 °C yielded $P_r = 0.68$ (Table 4, #6), which is within the margin of error indistinguishable from values of $P_r = 0.65$ – 0.71 obtained at room temperature and indicates that lower P_r values for **7b** might not be simply assigned to an increased tendency to stereoerrors. On the other hand, parallel polymerizations with **7b**/lactide ratios of 1:100, 1:200, and 1:400 under otherwise identical conditions (Table 4, #1, #3, and #5) showed P_r values between 0.65 and 0.71, independent of conversion or the **7b**/lactide ratio and rule out a simple competition of chain propagation and isomerization between rotamers as factors influencing the polymer microstructure. The exact mechanism of lactide polymerization with **7b** thus remains unclear at the moment.

Polymerizations with **7b** were also indifferent to the presence of THF, and comparable activities were obtained in the presence of 0, 10, 100, or 1000 equiv of THF (Table 5). In the presence of MeCN or pyridine, polymerization activity also decreased only slightly with Lewis base concentration. The value of P_r , however, increased upon addition of Lewis base. A comparable increase in stereoselectivity by chain-end control has been reported for *C_s*-symmetric magnesium and zinc diketiminate systems when the reaction solvent was switched from dichloromethane to THF.^{10,14} While the reasons for this increase are unclear in our case (and might be related simply to changes in solvent polarity), chain-end control on the polymer microstructure could not be diminished by preventing the coordination of the pending polymer chain with an additional Lewis base.

Summary and Conclusions

The use of aliphatic substituents on nitrogen allowed the synthesis of *C₂*-symmetric zinc diketiminate complexes, which were active initiators for the polymerization of *rac*-lactide. Alternating *R,R/S,S*-enchainment by chain-end control, previously observed for *C_{2v}*-symmetric diketiminato zinc complexes,⁸ still prevails for these complexes, and heterotactic PLA is obtained with **7a** and **7b**. The two chiral substituents in **7a** do not induce enantioselectivity in polymerization, which, judging from the facile rotation around the N–C bond found in the crystal structure of **7a**, indicates that the ligand framework is not sufficiently rigid and that its role is limited to provide sufficient steric bulk for heterotactic chain-end control.

For **7b**, reasons for the lack of isotactic enchainment remain unclear: fast isomerization, higher activity of the *meso*-isomer, or insufficient catalytic-site control might be

responsible. We are currently investigating if we can stabilize the lifetime of chiral rotamers and increase the steric differentiation in complexes comparable to **7b**.

Experimental Section

General Procedures. All reactions, except ligand synthesis, were carried out under an inert atmosphere using Schlenk and glovebox techniques under a nitrogen atmosphere. Zn(N(SiMe₃)₂)₂,³⁷ *S,S*-*nacnac*^{CH(Me)Ph}H,^{18,38} and *nacnac*^{Bn}H^{30,38} were prepared according to literature procedures. Solvents were dried by passage through activated aluminum oxide (MBraun SPS) and deoxygenated by repeated extraction with nitrogen. C₆D₆ was dried over sodium and degassed by three freeze–pump–thaw cycles. CDCl₃ and CD₂Cl₂ were dried over 4 Å molecular sieves. *rac*-Lactide (98%) was purchased from Sigma-Aldrich, kept at 5 °C, and used as received. All other chemicals were purchased from common commercial suppliers and used without further purification. ¹H and ¹³C NMR spectra were acquired on Bruker AMX 300, AV 400, or Avance 700 spectrometers. Chemical shifts were referenced to the residual signals of the deuterated solvents (C₆D₆: ¹H: δ 7.16 ppm, ¹³C: δ 128.38 ppm, CDCl₃: ¹H: δ 7.26 ppm). Elemental analyses were performed by the Laboratoire d'Analyse Élémentaire (Université de Montréal). Molecular weight analyses were performed on a Waters 1525 gel permeation chromatograph equipped with three Phenomenex columns and a refractive index detector at 35 °C. Chloroform was used as the eluant at a flow rate of 1.0 mL min⁻¹, and polystyrene standards (Sigma-Aldrich, 1.5 mg/mL, prepared and filtered (0.2 μm) directly prior to injection) were used for calibration.

S,S-*nacnac*^{CH(Me)Ph}ZnEt₂, **2a**. *S,S*-*nacnac*^{CH(Me)Ph}H, **1a** (250 mg, 0.82 mmol), and ZnEt₂ (136 mg, 1.1 mmol) were dissolved in toluene (8 mL) and stirred for 15 h at room temperature. Evaporation of the solvent and drying under fine vacuum yielded a yellow oil (86% yield), which contained less than 5% impurities according to NMR and was used without further purification.

¹H NMR (C₆D₆, 300 MHz, 298 K): δ 7.26 (d, *J* = 8 Hz, 4H, Ph), 7.14 (t, *J* = 8 Hz, 4H, Ph), 7.03 (t, *J* = 8 Hz, 2H, Ph), 4.70 (q, *J* = 7 Hz, 2H, CH(Me)Ph), 4.59 (s, 1H, CH(C=N)₂), 1.81 (s, 6H, Me(C=N)), 1.52 (d, *J* = 7 Hz, 6H, CH(Me)Ph), 1.08 (t, *J* = 9 Hz, 3H, ZnCH₂Me), 0.25 (q, *J* = 9 Hz, 2H, ZnCH₂Me). ¹³C {¹H} NMR (C₆D₆, 75 MHz, 298 K): δ 166.2 (C=N), 146.7 (*ipso* Ph), 128.7 (Ph), 126.7, 126.6, 96.1 (CH(C=N)₂), 57.9 (CH(Me)Ph), 24.3 (Me(C=N)), 22.9 (CH(Me)Ph), 12.0 (ZnCH₂Me), 5.57 (ZnCH₂Me).

nacnac^{Bn}ZnEt₂, **2b**. Diketimine **1b** (250 mg, 0.90 mmol) and ZnEt₂ (153 mg, 1.24 mmol) were dissolved in toluene (10 mL) and stirred for 15 h. The solvent was evaporated and the obtained yellow powder recrystallized from hexane at –30 °C (319 mg, 95%).

¹H NMR (C₆D₆, 300 MHz, 298 K): δ 7.10–7.14 (m, 8H, Ph), 7.00–7.05 (m, 2H, Ph), 4.67 (s, 1H, CH(C=N)₂), 4.51 (s, 4H, CH₂Ph), 1.75 (s, 6H, Me(C=N)), 1.28 (t, *J* = 9 Hz, 3H, ZnCH₂Me), 0.36 (q, *J* = 9 Hz, 2H, ZnCH₂). ¹³C {¹H} NMR (C₆D₆, 75 MHz, 298 K): δ 168.1 (C=N), 142.0 (*ipso* Ph), 128.8 (Ph), 127.1, 126.9, 96.8 (CH(C=N)₂), 55.0 (CH₂Ph), 21.9 (Me(C=N)), 13.1 (ZnCH₂Me), –1.93 (ZnCH₂Me). Anal. Calcd for C₂₁H₂₆ZnN₂: C, 67.38; H, 7.05; N, 7.54. Found: C, 67.96; H, 6.95; N, 7.50.

S-MeO₂CC(H)(Me)OZnEt₂, **3**. ZnEt₂ (204 mg, 1.63 mmol) and *S*-methyl lactate (169 mg, 1.63 mmol) were dissolved in toluene (10 mL) and stirred at room temperature for 15 min. Evaporation of the solvent and drying under vacuum yielded colorless, wax-like **3** (258 mg, 80%).

(37) Rivillo, D.; Gulyás, H.; Benet-Buchholz, J.; Escudero-Adán, E. C.; Freixa, Z.; van Leeuwen, P. W. N. M. *Angew. Chem., Int. Ed.* **2007**, *46*, 7247.

(38) El-Zoghbi, I.; Ased, A.; Oguadinma, P. O.; Tchirioua, E.; Schaper, F. *Can. J. Chem.*, submitted.

Table 6. Details of X-ray Diffraction Studies

	2a	4	6b	7a
formula	C ₂₁ H ₂₆ N ₂ Zn	C ₃₈ H ₄₂ N ₄ Zn	C ₂₅ H ₃₉ N ₃ Si ₂ Zn	C ₄₈ H ₆₄ N ₄ O ₂ Zn ₂
<i>M_w</i> (g/mol); <i>d</i> _{calcd.} (g/cm ³)	371.81; 1.314	620.13; 1.287	503.14; 1.219	859.77; 1.286
<i>T</i> (K); <i>F</i> (000)	150; 784	150; 1312	150; 536	150; 1824
cryst syst	triclinic	monoclinic	triclinic	orthorhombic
space group	<i>P</i> $\bar{1}$	<i>C</i> 2/ <i>c</i>	<i>P</i> $\bar{1}$	<i>P</i> 2 ₁ 2 ₁
unit cell: <i>a</i> (Å)	9.4077(6)	14.8210(3)	8.1588(2)	12.9219(3)
<i>b</i> (Å)	9.4416(6)	15.1994(3)	11.0074(2)	18.4221(4)
<i>c</i> (Å)	21.4629(14)	14.2091(3)	15.8174(3)	18.6609(4)
α (deg)	92.702(2)	90	90.658(1)	90
β (deg)	93.216(2)	90.010(1)	98.133(1)	90
γ (deg)	98.523(2)	90	102.576(1)	90
<i>V</i> (Å ³); <i>Z</i>	1879.4(2); 4	3200.89(11); 4	1371.18(5); 2	4442.20(17); 4
θ range (deg); completeness	2.1–72.6; 0.96	4.2–72.5; 0.99	2.8–63.5; 0.97	3.4–63.4; 1.00
collected reflns; <i>R</i> _{sigma}	24 585; 0.017	20 811; 0.021	18 435; 0.035	59 422; 0.040
indep reflns; <i>R</i> _{int}	7173; 0.026	3143; 0.033	4362; 0.038	7216; 0.052
μ (mm ⁻¹)	1.818; multiscan	1.303; multiscan	2.191; multiscan	1.642; multiscan
<i>R</i> ₁ (<i>F</i>); <i>wR</i> (<i>F</i> ²); GoF(<i>F</i> ²) ^a	0.037; 0.098; 1.07	0.031; 0.090; 1.09	0.032; 0.082; 0.97	0.029; 0.065; 0.97
residual electron density	0.46; -0.72	0.30; -0.28	0.26; -0.32	0.22; -0.38

^a *R*₁(*F*) based on observed reflections with *I* > 2 σ (*I*), *wR*(*F*²) and GoF(*F*²) based on all data.

¹H NMR (C₆D₆, 400 MHz, 298 K): δ 4.75 (q, *J* = 7 Hz, 1H, OCHMe), 3.29 (s, 3H, CO₂Me), 1.67 (d, *J* = 7 Hz, 3H, -OCHMe), 1.49 (t, *J* = 8 Hz, 3H, ZnCH₂Me), 0.48 (q, *J* = 8 Hz, 2H, ZnCH₂Me). ¹³C{¹H} NMR (C₆D₆, 101 MHz, 298 K): δ 178.1 (C=O), 70.4 (OCHMe), 52.0 (CO₂Me), 22.5 (OCHMe), 13.0 (ZnCH₂Me), 0.05 (ZnCH₂Me). Anal. Calcd for C₆H₁₂O₃Zn: C, 36.48; H, 6.12. Found: C, 36.28; H, 6.12.

nacnac^{Bn}Zn, **4**. Diketimine **1b** (250 mg, 0.900 mmol) and ZnEt₂ (56 mg, 0.45 mmol) were reacted in hexane (8 mL) for 15 h at room temperature. The residue obtained after evaporation of the solvent was washed with hexane and dried under vacuum to yield a colorless powder of **4** (113 mg, 41%).

¹H NMR (C₆D₆, 400 MHz, 298 K): δ 7.10–7.14 (d, *J* = 7 Hz, 4H, Ph), 7.04–7.10 (t, *J* = 7 Hz, 4H, Ph), 6.96–7.03 (t, *J* = 7 Hz, 2H, Ph), 4.43 (s, 1H, CH(C=N)₂), 4.14 (s, 4H, CH₃Ph), 1.71 (s, 6H, Me(C=N)). ¹³C{¹H} NMR (C₆D₆, 75 MHz, 298 K): δ 167.9 (C=N), 142.1 (*ipso* Ph), 128.3 (Ph), 127.5, 126.3, 94.2 (CH(C=N)₂), 54.2 (CH₃Ph), 22.0 (Me(C=N)). Anal. Calcd for C₃₈H₄₂N₄Zn: C, 73.60; H, 6.83; N, 9.04. Found: C, 73.37; H, 6.64; N, 8.96.

iPrOZnEt, **5**. ²⁶ZnEt₂ (50 mg, 0.40 mmol) and dry 2-propanol (24 mg, 0.39 mmol) were reacted in toluene (1.5 mL) for 12 h. The colorless powder obtained after evaporation of the solvent is used without further purification in subsequent reactions (46 mg, 85%).

¹H NMR (C₆D₆, 300 MHz, 298 K): δ 3.99 (sept, *J* = 7 Hz, 1H, OCHMe₂), 1.53 (t, *J* = 9 Hz, 3H, MeCH₂Zn), 1.18 (d, *J* = 7 Hz, 6H, OCHMe₂), 0.55 (q, *J* = 9 Hz, 2H, MeCH₂Zn). ¹³C{¹H} NMR (C₆D₆, 75 MHz, 298 K): δ 68.7 (OCHMe₂), 27.1 (2C, OCHMe₂), 12.8 (MeCH₂Zn), 1.61 (MeCH₂Zn).

S,S-nacnac^{CH(Me)Ph}ZnN(SiMe₃)₂, **6a**. Zn{N(SiMe₃)₂}₂ (993 mg, 2.57 mmol) and **1a** (750 mg, 2.45 mmol) were dissolved in hexane and stirred at room temperature for 24 h. Evaporation of the solvent yielded an orange, highly air-sensitive oil (989 mg, 76%) in 85–90% purity, which was used in subsequent reactions without further purification.

¹H NMR (C₆D₆, 300 MHz, 298 K): δ 7.25 (d, *J* = 7 Hz, 4H, Ph), 7.17 (t, *J* = 7 Hz, 4H, Ph), 7.04 (t, *J* = 7 Hz, 2H, Ph), 4.89 (q, *J* = 8 Hz, 2H, CH(Me)Ph), 4.55 (s, 1H, CH(C=N)₂), 1.84 (d, *J* = 8 Hz, 6H, CH(Me)Ph), 1.69 (s, 6H, Me(C=N)), 0.16 (s, 18H, SiMe₃). ¹³C{¹H} NMR (C₆D₆, 75 MHz, 298 K): δ 169.3 (C=N), 145.8 (*ipso* Ph), 128.8 (Ph), 126.5, 96.8 (CH(C=N)₂), 58.4 (CH(Me)Ph), 25.0 (Me), 24.0 (Me), 5.7 (SiMe₃). Anal. Calcd for C₂₇H₄₃N₃ZnSi₂: C, 61.00; H, 8.10; N, 7.90. Found: C, 63.33; H, 7.90; N, 6.92.

nacnac^{Bn}ZnN(SiMe₃)₂, **6b**. Zn{N(SiMe₃)₂}₂ (1.50 g, 3.88 mmol) and **1b** (1.08 g, 3.88 mmol) were dissolved in hexane (20 mL) and stirred for 12 h at room temperature. Evaporation of the solvent afforded an off-white powder, which was recrystallized from hexane (1.73 g, 89%).

¹H NMR (CDCl₃, 400 MHz, 298 K): δ 7.00–7.34 (m, 10H, Ph), 4.80 (s, 4H, PhCH₂), 4.72 (s, 1H, CH(C=N)₂), 2.04 (s, 6H, Me(C=N)), -0.20 (s, 18H, SiMe₃). (C₆D₆, 400 MHz, 298 K): δ 7.13–7.16 (m, 8H, Ph), 7.11–7.12 (m, 2H, Ph), 4.68 (s, 4H, PhCH₂), 4.64 (s, 1H, CH(C=N)₂), 1.71 (s, 6H, Me(C=N)), 0.13 (s, 18H, SiMe₃). ¹³C{¹H} NMR (C₆D₆, 75 MHz, 298 K): δ 170.2 (C=N), 141.0 (*ipso* Ph), 128.9 (Ph), 127.1, 126.9, 96.5 (CH(C=N)₂), 54.0 (PhCH₂), 22.1 (Me(C=N)), 5.2 (SiMe₃). Anal. Calcd for C₂₅H₃₉N₃ZnSi₂: C, 59.68; H, 7.81; N, 8.35. Found: C, 60.33; H, 7.71; N, 8.22.

S,S-nacnac^{CH(Me)Ph}ZnO*i*Pr, **7a**. Complex **6a** (200 mg, 0.38 mmol) was reacted with 2-propanol (23 mg, 0.38 mmol) in hexane (10 mL) for 20 h at room temperature. The solvent was reduced until the onset of precipitation. The solution was slightly warmed to redissolve any precipitate formed and kept for 24 h at -20 °C to yield colorless crystals of **7a** (90 mg, 55%).

¹H NMR (C₆D₆, 400 MHz, 298 K): δ 7.40 (d, *J* = 8 Hz, 4H, Ph), 7.19 (t, *J* = 8 Hz, 4H, Ph), 7.06 (t, *J* = 8 Hz, 2H, Ph), 5.05 (q, *J* = 7 Hz, 2H, CH(Me)Ph), 4.48 (s, 1H, CH(C=N)₂), 4.20 (sept, *J* = 6 Hz, 1H, OCHMe₂), 1.68 (d, *J* = 6 Hz, 6H, CH(Me)Ph), 1.67 (s, 6H, Me(C=N)), 1.275 (d, *J* = 7 Hz, 3H, OCHMe₂), 1.27 (d, *J* = 7 Hz, 3H, OCHMe₂). ¹³C{¹H} NMR (C₆D₆, 75 MHz, 298 K): δ 168.8 (C=N), 147.0 (*ipso* Ph), 128.4 (Ph), 126.6 (Ph), 126.2 (Ph), 96.2 (CH(C=N)₂), 66.0 (OCHMe₂), 57.8 (CH(Me)Ph), 28.96 (OCHMe₂), 28.91 (OCHMe₂), 24.8 (Me), 24.2 (Me). Anal. Calcd for C₂₄H₃₂N₂ZnO: C, 67.00; H, 7.50; N, 6.50. Found: C, 66.64; H, 7.40; N, 6.42.

nacnac^{Bn}ZnO*i*Pr, **7b**. Complex **6b** (1.00 g, 1.99 mmol) was dissolved in toluene (15 mL) and reacted with 2-propanol (152 μ L, 1.99 mmol) for 12 h at room temperature, during which some white precipitate appeared. The solvent was evaporated to a quarter of its volume and the obtained precipitate isolated by filtration. Recrystallization from hexane yielded colorless crystals (544 mg, 70%).

¹H NMR (CDCl₃, 300 MHz, 298 K): δ 7.05–7.24 (m, 10H, Ph), 4.45 (s, 4H, PhCH₂), 4.39 (s, 1H, CH(C=N)₂), 3.63 (sept, *J* = 7 Hz, 1H, OCHMe₂), 1.81 (s, 6H, Me(C=N)), 0.77 (d, *J* = 7 Hz, 6H, OCHMe₂). (C₆D₆, 400 MHz, 298 K): δ 7.24 (d, *J* = 7 Hz, 4H, Ph), 7.18 (t, *J* = 7 Hz, 4H, Ph), 7.08 (t, *J* = 7 Hz, 2H, Ph), 4.57 (s, 4H, PhCH₂), 4.52 (s, 1H, CH(C=N)₂), 3.95 (sept, *J* = 6 Hz, 1H, OCHMe₂), 1.71 (s, 6H, Me(C=N)), 1.08 (d, *J* = 6 Hz, 6H,

OCHMe₂). ¹³C{¹H} NMR (C₆D₆, 101 MHz, 298 K): δ 169.5 (C=N), 141.9 (*ipso* Ph), 128.5 (Ph), 127.0, 126.5, 94.3 (CH (C=N)₂), 66.5 (OCHMe₂), 54.1 (PhCH₂), 28.4 (OCHMe₂) 21.9 (*Me*(C=N)). Anal. Calcd for C₂₂H₂₈N₂ZnO: C, 65.75; H, 7.02; N, 6.97. Found: C, 65.85; H, 7.04; N, 6.88.

Typical Lactide Polymerization Conditions. A. Glovebox. In a glovebox, a solution of the desired catalyst in CH₂Cl₂ (1–2 mL) was added to a solution of *rac*-lactide in CH₂Cl₂ (5–10 mL). Typical conditions: [Zn] = 1.7–2.0 mM, Zn/lactide = 1:100 to 1:400, total volume: 6–12 mL. After stirring at ambient temperature (23 °C) for the desired time, the reaction or a reaction sample was quenched with 2 equiv of AcOH in CH₂Cl₂, removed from the glovebox, and freed from solvent immediately under vacuum. The obtained colorless PLA was either washed with EtOH to remove remaining monomer or dried without further treatment under vacuum and analyzed as a polymer/monomer mixture (determination of conversion).

B. Schlenk Line. In a Schlenk flask, a solution of the desired catalyst in CH₂Cl₂ (2 mL) was added via canula to a solution of lactide in CH₂Cl₂ (200–1000 mg, 10 mL). The resulting solution was stirred for the desired time, and reaction samples or final product was isolated as described above. For polymerizations at 0 °C, both solutions were cooled to 0 °C prior to addition.

C. J.-Young Tube. In a J.-Young tube, a solution of **7b** in CDCl₃ (26 mM, 75 μL, 1.9 μmol) was added by micropipet to a solution containing *rac*-lactide (75–82 mg), Lewis base

(< 40 μL), and CDCl₃ (1 mL). After short mixing, the tube was kept at ambient temperature and the reaction followed by NMR in the required intervals.

Microstructure Analysis. *P_r* values were determined from the integration of the methine region in homonuclear decoupled ¹H NMR spectra and calculated according to $P_r = 2I_1/(I_1 + I_2)$, with *I*₁ = 5.20–5.25 ppm (*rmr*, *mnr/rmm*), *I*₂ = 5.13–5.20 ppm (*mnr/rmm*, *mmm*, *mrm*).⁹ Resonances in ¹H and ¹³C spectra were assigned according to the literature.³⁹

X-ray Crystallography. Diffraction data were collected on a Bruker SMART 6000 with Montel 200 monochromator, equipped with a rotating anode source for Cu Kα radiation. Cell refinement and data reduction were done using APEX2.⁴⁰ Absorption corrections were applied using SADABS.⁴⁰ Structures were solved by direct methods using SHELXS97 and refined on *F*² by full-matrix least-squares using SHELXL97.⁴¹ All non-hydrogen atoms were refined anisotropically. Hydrogen atoms were refined isotropically on calculated positions using a riding model. Further experimental details are listed in Table 6 and given in the Supporting Information.

Acknowledgment. We thank Dr. Minh Tan Phan Viet and Sylvie Bilodeau for assistance with polymer NMR spectroscopy, Dr. Michel Simard for help with the structure of **2a**, Pierre Ménard-Tremblay for assistance with the molecular weight determinations, and Dr. Carole Fraschini for helpful discussions.

Supporting Information Available: Details of the crystal structure determinations (CIF). This material is available free of charge via the Internet at <http://pubs.acs.org>.

(39) Kasperczyk, J. E. *Macromolecules* **1995**, *28*, 3937. Kasperczyk, J. E. *Polymer* **1999**, *40*, 5455. Zell, M. T.; Padden, B. E.; Paterick, A. J.; Thakur, K. A. M.; Kean, R. T.; Hillmyer, M. A.; Munson, E. J. *Macromolecules* **2002**, *35*, 7700.

(40) APEX2, Release 2.1-0; Bruker AXS Inc.: Madison, WI, 2006.

(41) Sheldrick, G. M. *Acta Crystallogr.* **2008**, *A64*, 112.